International Journal of Scientific Research & Engineering Trends
Volume 10, Issue 5, Sept-Oct-2024, ISSN (Online): 2395-566X

Innovative Antenna Coupling Approaches for Low SAR in Smartphone Communication Modes

Associate Professor Dr TVS Divakar, Vambaravelli Mohini, Rupanagudi Siva Reddy
Department of Electronics and Communication Engineering,
GMRIT College ofEngineering, Rajam, Andhra Pradesh, India

Abstract- This paper provides a thorough investigation of coupling adjustment using two antennas in the speak position for voice conversations on recent smart phones. Using the optimal relative phase between components helps minimize SAR while maintaining efficiency through power splitting and appropriate interelement coupling. When not in talk position, antenna elements can remain used for MIMO without considerably lowering their fundamental limit of capacity, although this is of secondary significance. This approach is applicable to mobile communications frequencies ranging from 1.8 - 10. 8 GHz, given that the ground plane possesses the suitable form factor. This study shows that optimizing two PIFAs at 10.1 GHz may Reduce SAR by more than 50% over one element. SAR reduction remains consistent irrespective of the user's head structure or manipulation of the device while speaking.

Index Terms- Phased antenna array, Specific Absorption Rate (SAR)

I. INTRODUCTION

Over the last 30 years, mobile User Terminal devices have advanced in designing and its compactness. Guidelines have been established to limit the amount of electromagnetic field connected to the human head, calculated by Specific Absorption Rate. Initially, mobile devices were in different shapes, with an emphasis on positioning exterior whip antennas or designing interior planar antennas to minimize SAR. In the previous ten years, the extensive use of smartphones has necessitated to rethink how to reduce SAR for a wider yet thinner device. Latest smartphones use Multiple-Input and Multiple-Output transceiver technology required for both 4th and 5th generation cellular systems and Wi-Fi standards as mentioned in [1]. An innovative antenna design reduces SAR values by manipulating radiation fields at the air-tissue interface.[2] proposed 'reverse current' concept achieves impressive results, with measured SAR values below 1.0 W/kg and excellent antenna performance. As wireless communication systems densify and expand to meet growing demands, electromagnetic field exposure is expected to increase, raising public health concerns. This trend will be accelerated by the proliferation of connected devices and the adoption of new technologies like mmWave and massive MIMO is mentioned in [3]. A high-performance MIMO antenna system has been designed for 5G smartphones, featuring a wide bandwidth and high element-isolation. This innovative design enables reliable anti-interference performance and robustness in mobile devices in [4]. Understanding the electromagnetic energy uptake by the person body is essential for developing safe and efficient communication devices, with significant implications for industry and users shown in [5]. Phased array antennas are crucial for 5G mmWave communication, but mutual coupling can compromise their efficiency. [6] research addresses this issue through innovative design and simulation techniques, paving the way for improved 5G performance. A dual-band PIFA antenna is proposed in [7] featuring a compact design and suitable frequency range for wearable medical applications. Its performance is characterized by good impedance matching, low VSWR, and decent gain. A low-profile antenna design is proposed in [8] featuring a wideband PIFA with enhanced impedance bandwidth. The design combines multiple resonant modes, resulting in a significant improvement over traditional PIFA designs. A compact PIFA is developed in [9] and tested for biotelemetry use. Experimental results show reliable performance and low SAR levels making it suitable for implantable applications. A compact four-antenna module is designed for 5G terminals, featuring a circular arrangement of dual-mode PIFAs. Measured results in [10] show excellent performance, including wideband coverage and high isolation. However, due to the small amount of space in smartphones, these techniques are difficult to execute effectively. The phase between MIMO antennas has been found as a characteristic affecting. A SAR study of User Terminal with MIMO antennas revealed that the maximum SAR can be predicted based on the relative phase angle between antenna parts. This helps simplify conformance checks. This study found that the SAR of closely spaced and connected antennas varies significantly with phase. Additionally, power distribution across antenna elements can impact the SAR. Although relative phase and power distribution across antenna

© 2024 IJSRET

components can change SAR, the fundamental reason behind this phenomenon remains unclear. The SAR of the human head is reduced by sharing power between elements, superimposing fields, and adjusting current distribution based on coupling.

II. THEORY FOR ANTENNA REDUCTION SAR DESIGN

1. SAR Reduction and Antennas Mutual Coupling

Using two antennas in a cell phone helps lower SAR by dividing the overall power evenly between them. Optimizing the phase variation between elements reduces SAR by combining the penetrated fields near the surface. The phase variation between elements affects distribution of current, head- coupled fields, and SAR. Mutual coupling occurs when electro-magnetic energy is exchanged between nearest antenna elements. The scattering parameter S12 (or S21) is related to admittance parameters. Z0 represents the characteristic impedance, whereas Y11 and Y22 represent self-admittance at ports 1 and 2, respectively.

$$S_{12} = \frac{-2Y_{12}Z_0^2}{(1+Y_{11}Z_0)(1+Y_{22}Z_0) - Y_{12}Y_{21}Z_0^2}$$

To link Y12 =Y21 to the electric field of frequency f , uses the integral equation below

$$Y_{12}(f) = \frac{1}{V_1 V_2} \iiint_V (E_1(r_2;f).J_2(r_2;f))dV'$$

Where V1 and V2 are voltages. The strength of the emitted electrical field from first antenna to second antenna within a 3-D volume V is denoted by E1.

The infinitesimal dipole model is used to calculate the current distribution(J2) at 2nd antenna. Similarly, electric field from 2nd antenna affects the current distribution at 1st antenna.

When each antenna emits at the same time, the coupled current intensity to the opposing element and ground plane, as well as the driven current of each antenna, combine to substantially affect the current distribution of the entire User Terminal. This depends on the component's phase variation. The distribution of current impacts the surface magnetic field $H\,t\,p$ and penetrating electric field Ep on the head's surface, where brain tissue has a high permittivity,$\varepsilon\, r$.

$$E_p = \left(\frac{\mu_0}{\varepsilon_0 \varepsilon_r}\right) H_{tp}$$

where ε 0and μ0 represent the permittivity of free space and permeability of free space. All theories combine to reduce the input power received by each antenna element, resulting in decreased Ep1 and Ep2 penetration. The total field $E\,p\,T$ is determined by the relative phase of the components that superimpose together. Although components have substantial mutual coupling, changing the current distribution can lower $E\,p\,T$ even further. Hence, using density $M\,d$ and Conductivity ρ, the SAR is computed as

$$SAR = \frac{\rho \times |E_{pT}|}{M_d} (w/kg)$$

The SAR must follow National and International EMF exposure limits, which are 1.6 W/kg measured over 1 gram of body tissue from the FCC. The below remaining sections explain how the three developed concepts effectively reduce SAR within the acceptable limitations.

Geometry of the Designed Antenna

The designed PIFA contains three layers-Ground, Substrate and Patch. Table I displays dimensions of the designed antenna.

Table 1: Dimensions of the proposed design

Parameter Description	Parameter	Dimensions (in mm)
Substrate	Ls	25
	Ws	10.8
	ts	1.6
Ground	Lg	25
	Wg	10.8
	tg	0.035
Patch	Lp	20
	Wp	6
	tp	0.035
Feeding pin	Lf	5
	Wf	1

Model of the Design

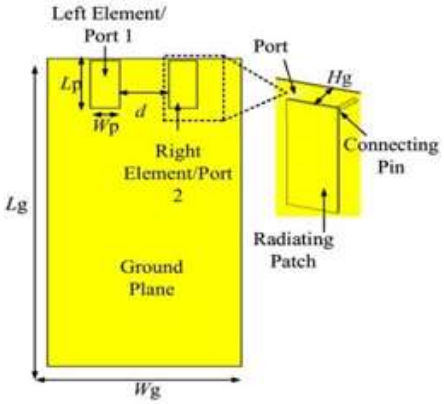

Fig 1: Visual of PIFA adjusted in a 2×2 MIMO arrangement

© 2024 IJSRET

Steps involved in the Prepared Model

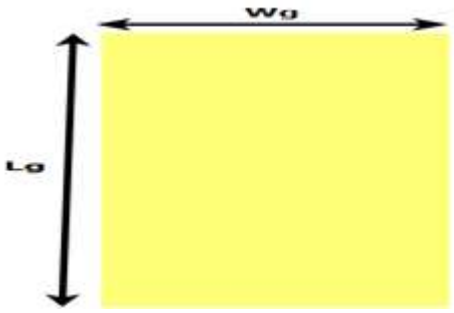

Fig 2: Ground

Fig 3: Substrate

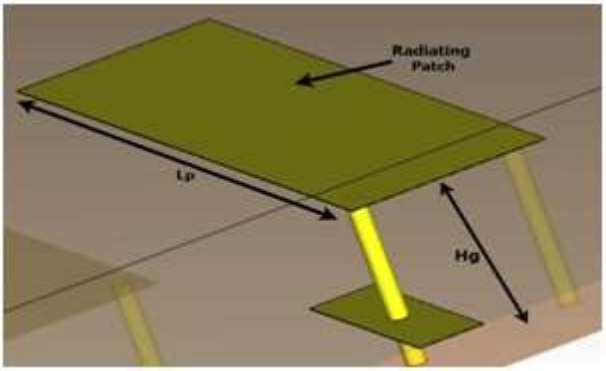

Fig 4: Patch

Fig (2) represents the bottom ground layer which is made up of copper material with the dimensions Lg x Wg mm^2. The simulations enable for the determination of the antenna's reflection coefficient, gain, co- and cross-polarizations, and surface currents. The recommended antenna operates in the 1.8 GHz to 10.8 GHz frequency range.

Fig (3) symbolizes the substrate layer between the ground and radiating element, which is made of Rogers RO3003(lossy) material and has dimensions of Ls x Ws mm^2. Substrate with low dielectric constants can help in reducing SAR by providing better radiation efficiency and lower near-field interaction with tissues.

Fig (4) The two radiating patches, made of copper (annealed) material, has dimensions of $L\ p$

$\times\ W\ p$ mm². It is responsible of effective transmitting and receiving of electromagnetic waves. Incorporating patches in PIFA designs helps to redistribute the current distribution on the antenna, effectively lowering the SAR values. This approach not only enhances the safety of the device by ensuring compliance with international SAR standards but also maintains the desired performance characteristics of the antenna.

Developed PIFA

Fig 5: Surface view

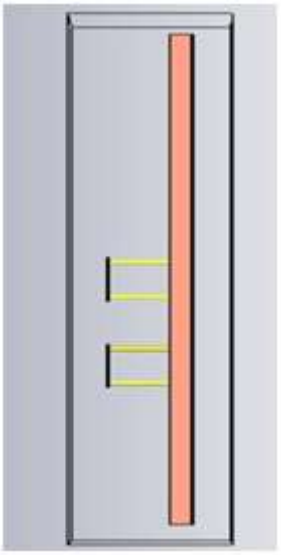

Fig 6: Down view

© 2024 IJSRET

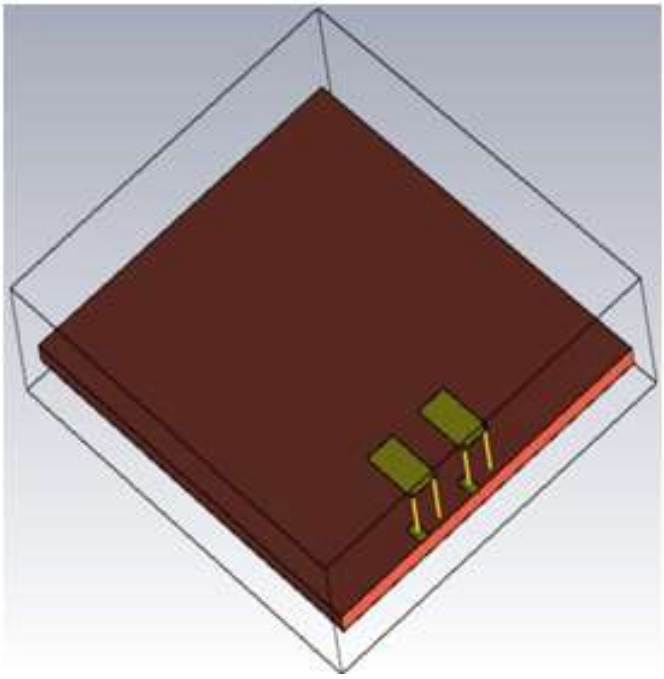

Fig 7: Overall view

III. FIELD ANALYSIS

The antenna's reflection coefficient, gain, co- and cross-polarizations, and surface currents can be calculated using simulations. The antenna operates between 1.8 GHz and 10.8 GHz, and the S11 parameter ensures a well-matched impedance spectrum. Figures 8, 9, 10 and 11 show measured E and H field radiation patterns for the antenna designed at 10.1 GHz, with radiation gain of 13dBi. Theta 'Θ' and phi 'Φ' are spherical coordinates for co- and cross-polarizations.

1. Electric-Field

Antenna electric fields increase in a horizontal direction. The patch and antenna feed lines generate the highest electric field. This is calculated in volts per meter. Fig 8 represents 6219 V/m electric field observations at resonate frequencies of 10.1 GHz.

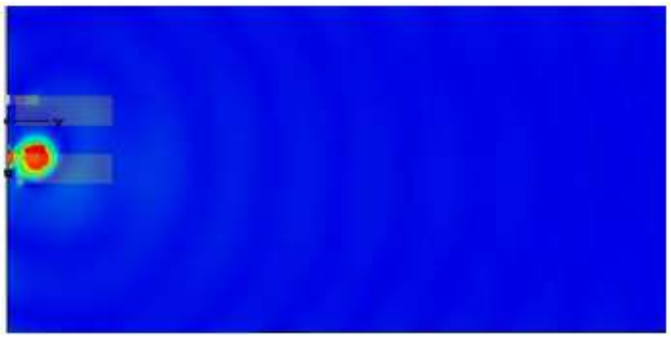

Fig 8: (a) E-Field at 10.1 GHz

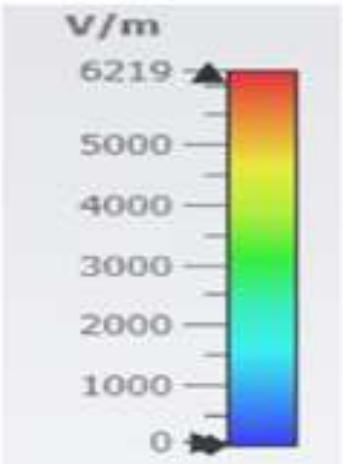

(b)E-field scale

2. Magnetic Field

An antenna's feed line and patch provide the most powerful magnetic field, which is measured in Amperes per meter. The Electric and Magnetic fields are typically perpendicular to each other. Fig 9 shows 2.98 A/m magnetic field observations at resonance frequencies 10.1 GHz.

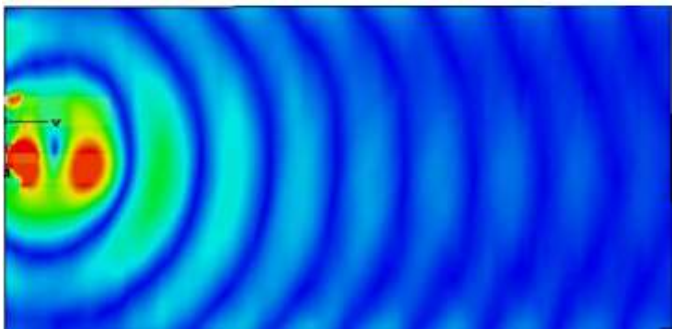

Fig 9: (a) H-Field at 10.1 GHz

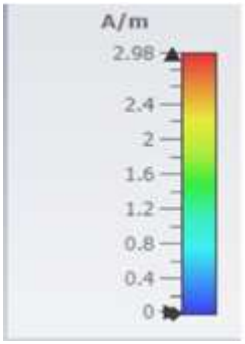

(b)H-Field Scale

3. Surface Current Field

The patch gets surface current from the feedline, which we measure in terms of Amperes per meter. A surface current of 6.21 A/m is created at 10.1 GHz, as illustrated in Fig 10

© 2024 IJSRET

Fig 10:(a) Surface current field at 10.1 GHz

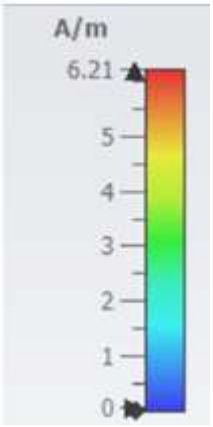

(b)Surface current field scale

4. Far Field

An antenna exhibits a far-field radiation pattern characterized by the presence of main, minor, side, and adjacent lobes, which indicate the directions of maximum gain. With a resonant frequency 10.1 GHz, the antenna obtains an output gain of 15.6 dBi. This far-field radiation pattern can be observed in Figures 11.

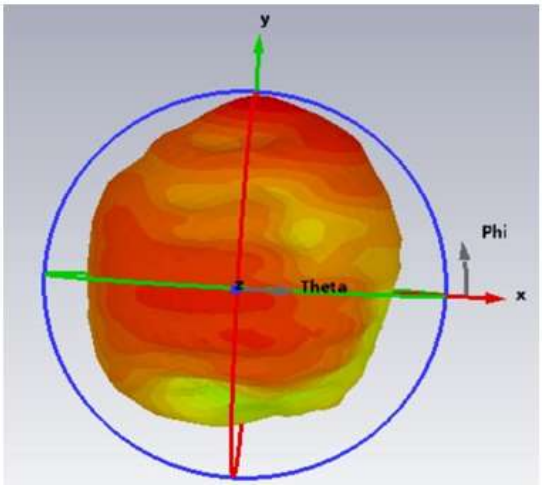

Fig 11: (a) Far field at 10.1 GHz

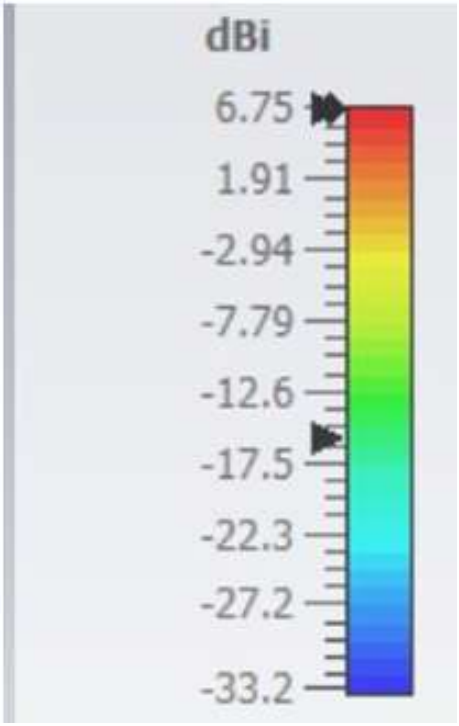

(b) Far field scale

IV. EXPERIMENTAL RESULTS AND DISCUSSION

The performance of the designed PIFA is assessed through design simulations. Figure 12 presents the reflection coefficient, while Figure 13 shows the VSWR values. Both readings align closely at a specific resonant frequency. Figures 14 and 15 illustrate the antenna's gain and efficiency, indicating that it operates effectively with minimal signal loss and reduces the SAR.

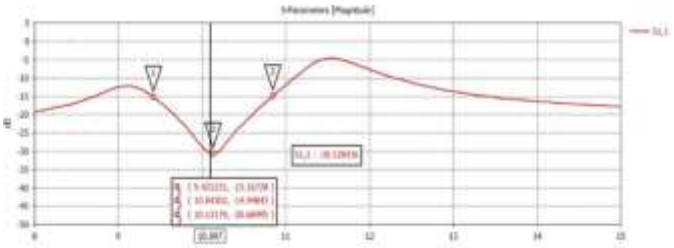

Fig 12: Frequency Vs Reflection Coefficient

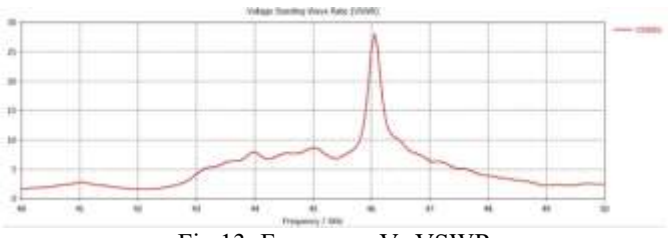

Fig 13: Frequency Vs VSWR

© 2024 IJSRET

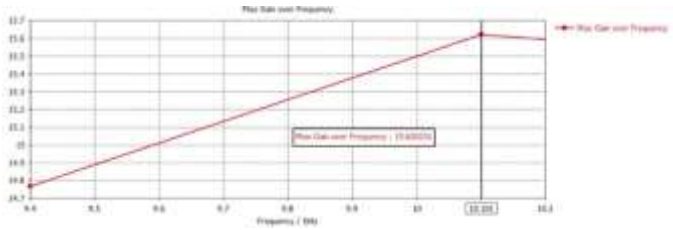

Fig 14: Maximum Gain Over Frequency

V. CONCLUSION

A PIFA, measuring 25 x 10.8 mm² with a fully covered copper ground plane, was simulated. The structure is fed by a microstrip line. Its enhanced E-field, H-field, and surface current resonant frequency make it ideal for reduction of SAR suitable for smartphones. The antenna features a bandwidth ranging from 1.8 -10.8 GHz and a calculated 15.6 dBi gain. The simulated VSWR and reflection coefficient characteristics were found to be highly accurate. By dispersing the source power in two directions and adjusting the phase variation between the two antennas, the deep fields can superpose and form the least magnitude. Furthermore, when they are enough near together, they can benefit from coupling. Optimizing a single element can lower SAR by up to three times. This works consistently regardless of head position or user handling, all in all the earpiece is assumed to be against the ear.

REFERENCES

1. Muhammad Ali Jamshed, Member, IEEE, Tim W. C. Brown, Member, IEEE, and Fabien Héliot, Member, IEEE. “Dual Antenna Coupling Manipulation for Low SAR Smartphone Terminals in Talk Position”, IEEE Transactions on Antennas and Propagation, Vol. 70, No. 6, June 2022.
2. Huan Huan Zhang , Member, IEEE, Guo Guo Yu, Ying Liu, Member, IEEE, Yi Xiang Fang, Guangming Shi, Senior Member, IEEE and Shang wang, “Design of Low-SAR Mobile Phone Antenna: Theory and Applications”, IEEE Transactions on Antennas and Propagation, Vol. 69, No. 2, February 2021.
3. X.-T. Yuan, W. He, K.-D. Hong, C.-Z. Han, Z. Chen, and T. Yuan, “Ultra-wideband MIMO antenna system with high element-isolation for 5G smartphone application,” IEEE Access, vol. 8, pp. 56281–56289, 2020.
4. Muhammad Ali Jamshed, Student Member, IEEE, Fabien Héliot, Member IEEE, Tim W. C. Brown, Member, IEEE. “A Survey on Electromagnetic Risk Assessment and Evaluation Mechanism for Future Wireless Communication Systems”, IEEE Journal of Electromagnetics, RF, and microwaves in medicine and biology, Vol.4, No.1, March 2020.
5. Hanyang Wang (Senior Member, IEEE). “Analysis of Electromagnetic Energy Absorption in the Human Body for Mobile Terminals”, IEEE open journal of Antennas and Propagation, Vol 1, 2020.
6. TVS Divakar, B. Vijay Gowtham Raju, D. Pradeep, A. Pavan Kalyan, B. Tarun Kumar. “Design and Analysis of Phased Antenna Array for 5G Communication”, 2023 JETIR April 2023, Volume 10, Issue 4.
7. T.V.S. Divakar, P. Krishna Rao, A. Sudhakar, “Miniaturised Edge Slotted Dual Band PIFA Antenna for Wearable Medical Applications at 2-9 GHz”, IEEE Antennas and Wireless Propagation Letters, Vol. 16, pp-2550 2553-(2023).
8. Rongling Jian, Yueyun Chen, and Taohua Chen, “A Low-Profile Wideband PIFA Based on Radiation of Multiresonant Modes”, IEEE Antennas and Wireless Propagation Letters, Vol.19, No.4, April 2020.
9. Muhammad Solihin Zulkefli, Kai Zhang , Mariella Sarestoniemi William G. Whittow and Ping Jack Soh, Senior Member, IEEE, SamiMyllymäki , Senior Member, IEEE, SenYan , Member, IEEE, Senior Member, IEEE. “Experimental Wireless Link and SAR Assessments of an Implantable PIFA for Biotelemetry in the 2.45 GHz Band”, IEEE Journal of Electromagnetics, RF, and microwaves in medicine and biology, Vol.7, No.3, September 2023.
10. Le Chang, Member, IEEE, and Hanyang Wang, Fellow, IEEE, “Miniaturized Wideband Four-Antenna Module Based on Dual-Mode PIFA for 5G 4 × 4 MIMO Applications”, IEEE Transactions on Antennas and Propagation, Vol. 69, No. 9, September 2021.

© 2024 IJSRET